

© Copyright 1999 American Meteorological Society (AMS). Permission to use figures, tables, and brief excerpts from this work in scientific and educational works is hereby granted provided that the source is acknowledged. Any use of material in this work that is determined to be “fair use” under Section 107 of the U.S. Copyright Act or that satisfies the conditions specified in Section 108 of the U.S. Copyright Act (17 USC §108, as revised by P.L. 94-553) does not require the AMS’s permission. Republication, systematic reproduction, posting in electronic form on servers, or other uses of this material, except as exempted by the above statement, requires written permission or a license from the AMS. Additional details are provided in the AMS CopyrightPolicy, available on the AMS Web site located at (<http://www.ametsoc.org/AMS>) or from the AMS at 617-227-2425 or copyright@ametsoc.org.

Permission to place a copy of this work on this server has been provided by the AMS. The AMS does not guarantee that the copy provided here is an accurate copy of the published work.

4.3

THE GROWTH AND DECAY STORM TRACKER ¹

M.M. Wolfson,² B.E. Forman, R.G. Hallowell, and M.P. Moore
Massachusetts Institute of Technology
Lincoln Laboratory
Lexington, Massachusetts

1. INTRODUCTION

A new method for tracking storms that accounts for systematic growth and decay has been developed by MIT Lincoln Laboratory under the FAA Aviation Weather Research Program's Convective Weather Product Development Team. The team includes scientists and engineers from the National Center for Atmospheric Research (NCAR), the National Severe Storms Laboratory (NSSL), and MIT Lincoln Laboratory (MIT LL). Predicting convective weather is extremely important to aviation, since at least half of the national airspace delay is caused by thunderstorms. Accurate 1-hour convective weather forecasts meet critical terminal traffic planning needs of the TRACON and ARTCC supervisors and traffic managers (Forman, *et al.*, 1999).

This new technique automatically tracks the storm envelope instead of the individual cells, which has been a classic problem in radar meteorology. By effectively tracking the storm forcing, we account for systematic growth and subsequent decay. Quantitative scoring has shown that this approach is better at forecasting regions of heavy precipitation 30-60 min in advance than contemporary extrapolation techniques. Based on this promising performance, the technique is being operationally evaluated in real-time at Dallas/Ft. Worth International Airport as part of the Integrated Terminal Weather System (ITWS) prototype operating there (Hallowell, *et al.*, 1999), and in a national demonstration operated for a limited number of airlines by NCAR (Mueller, *et al.*, 1999). Also, NSSL is investigating this technique for possible inclusion in future builds of the NEXRAD software.

2. BACKGROUND

Byers and Braham (1949) broadly categorized thunderstorms into two categories: "airmass" and "line" storms (Figure 1). More recently, Weisman and Klemp (1986) defined the categories as "single cell," "multicell," and "supercell" storms. Airmass or single cell storms are

small scale, seemingly random, fairly disorganized convective elements. Line storms or multicell storms are a collection of cells much like airmass cells, but they are maintained in an organized linear pattern, or "envelope." Line storms maintain this pattern because they are typically forced at a large scale by a frontal discontinuity (e.g., boundary between cold and warm air masses or between dry and moist air masses), large gravity waves, a sea breeze front, or the gust fronts from neighboring decaying cells. In the summer months, the percentage of line storms is large in the north, while airmass storms are predominant in the southeast. Line storms tend to dominate everywhere during the spring, fall and winter months. Through our assessment of user needs, Forman, *et al.*, (1999) found that line storms tend to cause the most significant air traffic safety and delay threat. Fortunately, they also turn out to be the most predictable types of storms.

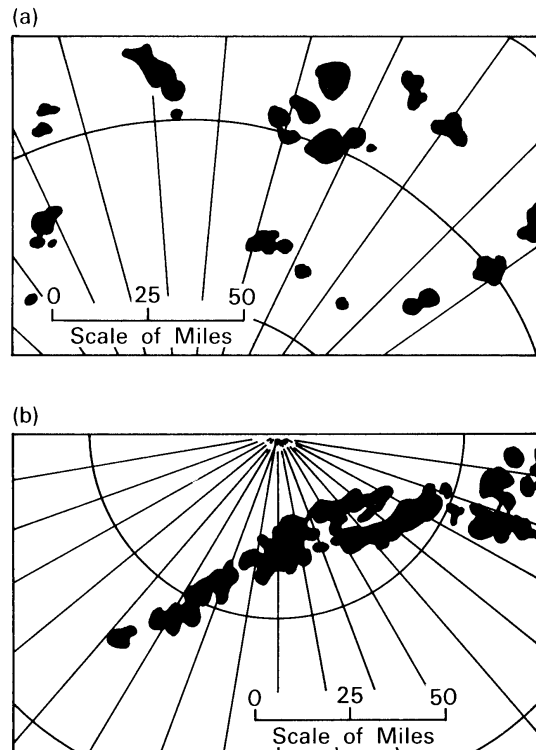


Figure 1. (a) Radar echoes on a day of random air mass thunderstorms. (b) Radar echoes on a day of squall line thunderstorms. The radial lines and arcs indicate the azimuths and ranges from the radar site. (Redrawn from Byers and Braham, 1949).

¹ This work was sponsored by the Federal Aviation Administration. The views expressed are those of the authors and do not reflect the official policy or position of the government.

² Corresponding author address:
Dr. Marilyn M. Wolfson; MIT Lincoln Laboratory;
244 Wood St. Lexington, MA 02420-9185.
Email: mwolfson@ll.mit.edu
Phone: 781-981-3409 Fax: 781-981-0632

Wilson (1966) showed that strong, large scale storms in the atmosphere are inherently more persistent with time than small scale storms, and he reminded us of this in his invited speech at the 1997 Convective Weather Forecasting Workshop (7th Conference on Aviation Weather, AMS). Since 1966, many other researchers have confirmed Wilson's findings. For example, Browning, *et al.* (1982) noted that "individual convective rain echoes several kilometers across tended to be predictable for only 10 min or so, whereas echoes associated with mesoscale precipitation areas and rainbands 50 km across were predictable for over an hour."

Large scale organized storms are made up of clusters of single cells which are themselves short-lived. As these multicell storms propagate, new storms grow (often along a preferred flank), and old storms decay. The net storm motion is a result of this discrete propagation, and is often very different from the individual cell motion (e.g., Marwitz, 1972). Wilson (1966) found that cells tended to move with the mean wind between 10Kft and 20Kft, but that "large-scale features move more slowly and to the right of the small-scale features."

Determining the envelope motion separate from the storm cell motion is a long-standing problem in weather radar research (e.g., Chornoboy *et al.*, 1994). Forecasts of future storm locations are typically made by extrapolating the motion of individual cells, using either a cross-correlation or centroid tracking technique. For very short-term predictions, this cell motion is accurate, but for longer-term predictions, the envelope must be tracked.

3. DETERMINING ENVELOPE MOTION

To determine the motion of the long-lived storm elements, the large-scale signal must be extracted and tracked. The separation of the large-scale component from the full scale can be accomplished by filtering techniques. Browning (1979) used a large-scale filtering step in his FRONTIERS forecasting process. He degraded the data from 5x5 km pixels to 20x20 km, and reintroduced some major storm cores after the patches had been advected. Bellon and Zawadzki (1994) used an area-averaging technique to reduce rms errors in rainfall accumulation forecasts, and derived an empirical relationship between the scale of the filtering and the forecast time interval. The filters used in all of these studies were square, with aspect ratio equal to one.

Boundary layer forcing for convection tends to organize storms in regions that are often 3-4 or more times longer than they are wide. To match this geometry, our approach uses an elliptical filter to extract the large-scale signal. A large square filter would over-filter in the cross-front direction, but the elliptical filter allows us to extract these long narrow large-scale regions with a high degree of long-front filtering.

A preliminary qualitative study to determine the optimal filter size and aspect ratio for large-scale

features of organized storms was performed on a suite of 12 cases from Memphis, Dallas and Orlando. Filters with sizes (in km) of 5x15, 9x27, 15x45, 15x61, 21x105 and 37x181, having aspect ratios of 3:1, 4:1, and 5:1, were tested. The results showed that a filter with an approximate size of 15x61 km and an aspect ratio of 4:1 best approximated the large-scale features of the organized storms tested. When tests were performed on 4 km data, the optimal filter size had the same 4:1 aspect ratio, but slightly different dimensions: 5x21pixel (20x84 km). More extensive quantitative testing to optimize filter size and aspect ratio vs. forecast time interval is currently in progress.

The elliptical filter is applied to the Vertically Integrated Liquid water (VIL) field, or any other weather radar data to be tracked. For data with 4-km resolution, the 5x21 filter is applied at every valid data point in the image according to the following steps:

1. The center point of the filter overlays a point in the original unfiltered image. The average of all the image points that underlay the filter pixels (light grey in Figure 2) is computed.
2. The filter is then rotated through 180° in equal increments (we use 10°), and the maximum of the average value at each rotation is assigned to the corresponding point in the filtered image.

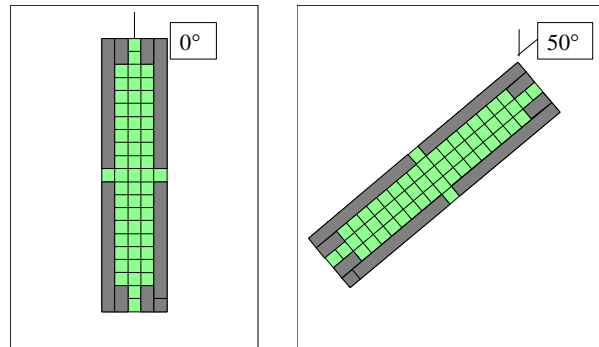


Figure 2. (Left) The 5x21 pixel elliptical filter used on 4 km data. The initial orientation of the filter is vertical. (Right) The filter is rotated in 10° increments (illustrated here at 50°), to determine the maximum average filter value.

To illustrate the effect of elliptical filtering, we have selected a line storm case from 1 June 1996 in Dallas, where the envelope motion and cell motion were quite different. Figure 3 shows the unfiltered "full-scale" image (VIL), the large-scale image (derived with the 15x61 km elliptical filter), and the small-scale image (derived by subtracting the result of a 15x15 km filter from the unfiltered image, thus selecting all scales less than 15x15 km). Within the large and small-scale images the storm motion vector resulting from correlation tracking is shown. The large-scale signal is moving southeast at 34 knots, while the small-scale signal is moving northeast at 21 knots.

To examine the relative longevity of the large-scale and small-scale components, we plotted the percentage of pixels with high correlation (>0.5) between successive images for this case. Figure 4 confirms that large-scale components decorrelate less rapidly with time, and thus are longer-lived than the small-scale components.

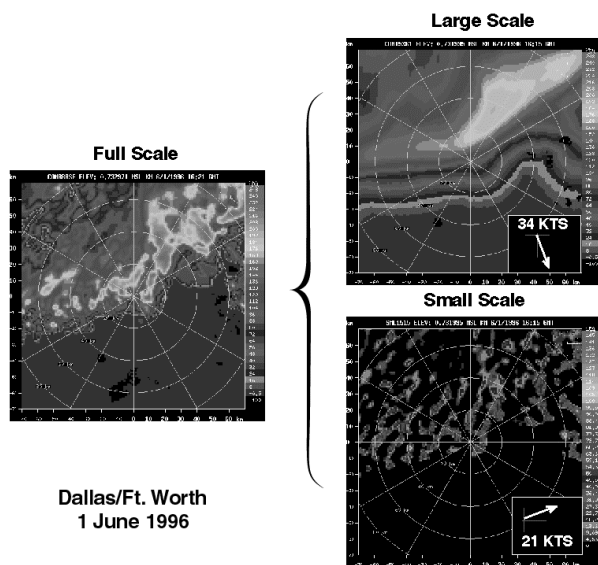


Figure 3. (Left) The result of filtering full scale image to produce large scale and small scale images. The motion of the large scale and small scale components, found with a correlation tracker, are indicated.

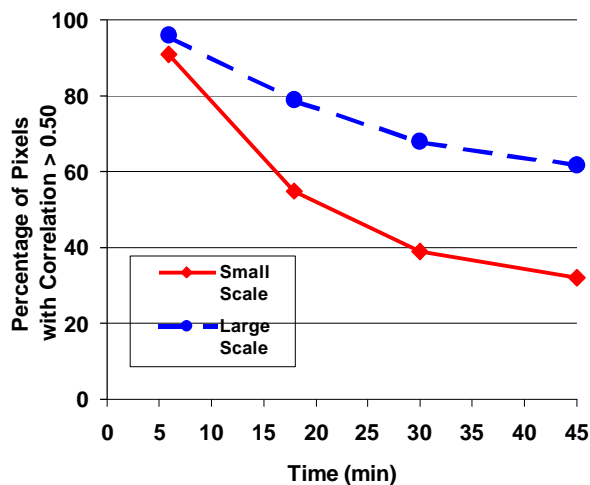


Figure 4. The relative longevity of large-scale and small-scale components of the 1 June 1996 storm is illustrated. The percentage of pixels with correlation >0.5 is used as a measure of persistence.

The large-scale propagates to the southeast by virtue of new cells growing preferentially on the southeast side of the line and old cells decaying on the northwest side. We have dubbed this new elliptical filter/tracker the “Growth and Decay Storm Tracker³” because it can account for this type of systematic growth and decay.

4. PERFORMANCE RESULTS

The performance of the Growth and Decay Storm Tracker depends on several variables, in addition to the advection and scoring methods. These are: a) the size and shape of the filter, b) the performance of the cross-correlation tracker, c) the time interval between successive scans that are correlated to determine storm motion, d) the forecast lead time (e.g., 30-min, 60-min, etc.), and e) the type of storm being tracked. In this section, quantitative results are presented for the latter three variables.

The ITWS cross-correlation tracker is used to derive storm motion, with optimized parameter settings for the 60-min forecast problem [Table 1; MIT LL (1998)]. In each of the following experiments, we compare the case of no filtering with the large-scale filtered data. For each data type we tracked 5 levels of data: for VIL, the levels were: 0.76, 3.5, 6.9, 12.0, 32.0 kg/m², corresponding to VIP levels 2-6; for large scale, a histogram was used to determine the tracking levels at 60%, 70%, 80%, 90%, and 95% populations. The resulting storm motion vectors were used to advect the unfiltered data forward in time. This advected data was compared with the true data 60 min later to determine forecast performance. Both the advection and scoring methodologies are described by Hallowell, *et al.* (1999). Performance is measured by Critical Success Index (CSI), computed as:

$$CSI = Hits / (Hits + Misses + False Alarms)$$

Table 1. ITWS Correlation Tracker settings.

Correlation Tracker	4 km	1km
Speed limit (pixels/min)	0.9	3.6
Correlation box size (pixels)	8x8	14x14
Min/Max valid weather (%)	10/90	10/90
Global constraint	±70°	±70°
Time averaging	0.25	0.25
Minimum correlation	0.55	0.55

The first experiment is designed to show the effect of large scale filtering at 1 km (15x61 pixel filter) and 4 km (5x21 pixel filter) resolution, compared with the benefit of increased time interval between correlation pairs. NEXRAD data for 1 June 1996 in DFW is used, and each scan is 6 min. Table 2 presents the performance results for 60-min forecasts.

³ Patent has been applied for by Massachusetts Institute of Technology.

Table 2(a). CSI results for 1-km data.

	1 scan	2 scans	3 scans
Large scale	26.15	31.47	34.38
Unfiltered	4.40	11.36	31.74

Table 2(b). CSI results for 4-km data.

	1 scan	2 scans	3 scans
Large scale	35.32	45.67	47.64
Unfiltered	17.60	30.96	44.03

First, all scores are higher at 4-km resolution than at 1-km, because a) the increased pixel size is providing some filtering of small, evanescent components, and b) the 5x5 pixel verification covers 400 km² at 4-km and 25 km² at 1-km. All scores improve with increasing time interval between successive images, but they vary much less drastically for the large-scale filtered case. The large CSI point jump for 4-km data between 1 and 2 scans is due to improved resolution of the storm motion. Even a fast-moving line storm moves less than 1-pixel in 6-min (1 scan), so quantization errors are reduced by increasing this time interval.

The poor unfiltered data scores at 1 and 2 scans reflect the tracking and correlation of cells within the line. At the 3-scan difference (18-min), the original cells have largely decayed and new ones have grown, leading to an unfiltered correlation track vector much closer to the envelope motion. The motion of the line storm in this particular case is very steady, so the detriment of going to longer time intervals is not illustrated here. In rapidly evolving storm cases, the best choice is a shorter time interval between scans. Based on experiments with many different types of storm cases from different regions of the country, we determined that an interval of 2 scans is the most robust for a 1-hour forecast, although this can be a site adaptable (perhaps seasonal) parameter in any operational system. All following results were derived using a 12-min (2 scan) time interval for cross correlation.

The second experiment compares the unfiltered and large-scale tracker performance at a variety of forecast lead times. The results for 10, 20, 30, and 60 min are shown in Table 3. At 10 min, the scores are virtually identical because a) the storm has not evolved much, and b) the forecast is not advected far from the truth in either case. Differences begin to arise at 20 min and grow with time, as the unfiltered data tracker moves the entire pattern according to the cell motion and the large-scale tracker according to the envelope motion.

Table 3. CSI results for different forecast lead times.

Fcst Time:	10 min	20 min	30 min	60 min
Large scale	84.00	71.42	61.30	45.67
Unfiltered	82.98	65.17	50.28	30.96

The data case of 1 June 1996 was selected precisely because the cell motion and envelope motion were very different. In most cases the large-scale and full-scale results do not differ quite this much. The third experiment shows a comparison of the 60-min CSI forecast scores from several different storm cases. The 9 June 1994 case is a memorable bow-echo storm that occurred during the ITWS demonstration in Memphis. The 24 July 1996 Memphis storm was studied by the Convective Weather PDT during their collaborative data collection that year (Mueller, Wolfson, and Eilts, *et al.*, 1997). The other two cases were both selected from our 1998 live demonstration in Dallas: one is a highly predictable line storm and the other is a fairly unpredictable air mass storm.

The results in Table 4 illustrate the wide range of 60-min forecast scores for different storm types, and the different performance of the unfiltered vs. large-scale tracking. Although on average the large scale filtering (Growth and Decay Storm Tracker) provides a ~20% performance increase for this collection of cases, one could find a set of cases (or a subset of times for these cases) for which it made more or less difference. The filtering is most valuable in cases in which a) there is some large scale organization (absent in many airmass cases) and b) the systematic storm growth and decay causes discrete propagation of the storm complex (envelope) in a direction different from the cell motion.

Table 4. CSI results for 60-min forecast for several cases.

Date Airport	Case description [duration scored]	Large scale	Unfiltered
6/1/96 DFW	Strong, extended line storm; very steady. [5.2 hrs.]	45.67	30.96
6/9/94 MEM	Bow Echo case, "Day All Hell Broke Loose II" [4 hrs.]	40.32	32.45
7/24/96 MEM	Air mass storms, with some organization due to colliding gust fronts. [6 hrs.]	27.55	21.83
6/4/98 DFW	Explosive growth, multiple moderate strength lines. [6 hrs.]	59.95	57.53
8/18/98 DFW	Slow moving air-mass storms. [5 hrs.]	22.05	17.67

5. SUMMARY

The dialogue on storm nowcasting in this country over the past 5-10 years has largely centered on making accurate 30-min forecasts, often in weakly forced synoptic situations where storms are typically small and short-lived (Wilson and Mueller, 1993). Forecasting airmass storms is a very difficult scientific problem, requiring detailed atmospheric boundary layer

observations and the use of sophisticated numerical models.

The Convective Weather Product Development Team has approached the problem of convective weather forecasting by first researching the specific needs of aviation users (Forman, *et al.*, 1999). We learned that large scale organized storms (line storms) cause the most serious problem for aviation. In focusing on these events, we found many cases for which a reasonably useful 60-min forecast could be made. We also discovered several examples where conventional cell tracking failed because of differences between storm cell and envelope motion. By extracting the large, persistent scales from the storms with an elliptical filtering technique, it was possible to automatically determine the storm envelope motion for these failure cases.

The Growth and Decay Storm Tracker can account for systematic growth and decay in organized storms, but cannot predict large changes in the storm spatial extent or envelope pattern. Techniques for anticipating convective initiation and large-scale decay, which could both improve the 60-min forecast scores and allow extension of the forecast lead-time to 90-120 min, are currently under investigation. Our goal is to provide an operationally useful capability within the next 1-2 years that could be considered for implementation within the ITWS and WARP (Weather and Radar Processor) preplanned product improvement programs.

6. REFERENCES

- Bellon, A. and I. Zawadzki, 1994: Forecasting of hourly accumulations of precipitation by optimal extrapolation of radar maps. *Journal of Hydrology*, **157**, 211-233.
- Browning, K.A., 1979: The FRONTIERS plan: a strategy for using radar and satellite imagery for very-short-range precipitation forecasting. *The Meteorological Magazine*, **108**, 161-184.
- Browning, K.A., *et al.*, 1982: On the Forecasting on Frontal Rain Using a Weather Radar Network. *Mon. Wea. Rev.*, **110**, 534-552.
- Byers, H.R., and R.R. Braham, 1949: The Thunderstorm. U.S. Government Printing Office, Washington, DC, 287 pp.
- Chornoboy, E.S., A.M. Matlin, and J.P. Morgan, 1994: Automated Storm tracking for Terminal Air Traffic Control. *The Lincoln Laboratory Journal*, **7**, 427-448.
- Forman, B.E., *et al.*, 1999: Aviation User Needs for Convective Weather Forecasts. 8th Conf. On Aviation Meteorology, this volume.
- Hallowell, *et al.*, 1999: The Terminal Convective Weather Forecast Demonstration at the DFW International Airport, 8th Conf. On Aviation Meteorology, this volume.
- Marwitz, J.D., 1972: The structure and motion of severe hailstorms. Part II. Multicell storms. *J. Appl. Meteor.*, **11**, 180-188.
- MIT Lincoln Laboratory, 1998: Integrated Terminal Weather System (ITWS) Algorithm Description. Chapter 15: Storm Motion/Storm Extrapolated Position. Rev. B. DOT/FAA/ND-95/11. LL Project Report No. ATC-255.
- Mueller, C.K., *et al.*, 1999: National Convective Weather Forecast Product. 8th Conf. On Aviation Meteorology, this volume.
- Mueller, C.K., *et al.*, Wolfson, M.M., *et al.*, and Eilts, M.D., *et al.*, 1997: The Memphis ITWS Convective Forecasting Collaborative Demonstration. 7th Conf. On Aviation Meteorology, Long Beach, CA., 249-257.
- Weisman, M.L., and J.B. Klemp, 1986: Characteristics of Isolated Convective Storms. Chapter 15, *Mesoscale Meteorology and Forecasting*, Ed. by P.S. Ray., 331-358.
- Wilson, J.W., 1966: Movement and predictability of radar echoes. NSSL Tech Memo, No. 28, Norman, OK. 30 pp.
- Wilson, J.W., and C.K. Mueller, 1993: Nowcasts of Thunderstorm Initiation and Evolution. *Weather and Forecasting*, **8**, 113-131.